Supporting Information

Exploring the role of viologen and iodocuprate on enhanced resistive switching performance of Anderson polyoxometalate-based three-component hybrids

Huai-Bin Chen,[a] Mei-Yun He,[a] Tao Li,[a] Chu-Chu Deng,[a] Hui-Ping Xiao,[a] Ming-Qiang Qi,[b] Xiang-Jian Kong,[b] Hao-Hong Li,[a,*] Xin-Xiong Li[a,*] and Shou-Tian Zheng[a,*]

[a]Fujian Provincial Key Laboratory of Advanced Inorganic Oxygenated Materials, College of Chemistry, Fuzhou University, Fuzhou, Fujian, 350108, China.

[b]State Key Laboratory of Physical Chemistry of Solid Surface, College of Chemistry and Chemical Engineering, Xiamen University Xiamen, 361005, China.

Corresponding authors, E-mail address: lihh@fzu.edu.cn, lxx@@fzu.edu.cn, stzheng@fzu.edu.cn

Contents

Section 1: Experimental Section

Materials and General methods: $(TBA)_3MnMo_6O_{18}(L)_2 \cdot 2CH_3CN$ precursor was prepared as described in the literature,[1] and 2-(Hydroxymethyl)-2-(pyridine-4-yl)-1,3-propanediol (**H_3L**) was synthesized with literature method.[2] All other chemicals were commercially purchased and used without further purification. IR spectra were recorded on an Opus Vertex 70 FT-IR infrared spectrophotometer in the range of 400~4000 cm^{-1}. Thermogravimetric analysiswas performed on a Mettler Toledo TGA/SDTA 851e analyzer under an air-flow atmosphere with a heating rate of 10 ºC/min in the temperature of 30~1000 ˚C. PXRD patterns were obtained by using a Ultima IV diffractometer with Cu-Kα radiation (λ = 1.5418 Å) in the range 5~ 45°. UV-vis adsorption spectra were collected using a PerkinElmer Lambda 35 spectrophotometer to monitor the release process. Cyclic voltammetry (CV) was performed with a CHI660E electrochemical workstation by using of a conventional three-electrode cell. The HR-SEM images were taken on a Verios G4 field-emission scanning electron microscope. Electrical bistability measurement on ITO/POMOF/Ag device was executed on KEYSIGHT B2911A single channel digital source meter. Single-crystal X-ray diffraction data for **1**, **2** and **3** were collected on a Bruker APEX II diffractometer at 175 K equipped with a fine focus, 2.0 kW sealed tube X-ray source (MoK radiation, λ = 0.71073 Å) operating at 50 kV and 30 mA.

Synthesis

$(MV)_3(MnMo_6O_{18}L_2)_2 \cdot 4DMF$ (1): A mixture of $(TBA)_3[MnMo_6O_{18}L_2] \cdot 2CH_3CN$ (0.274 g, 0.20 mmol), $MV \cdot Cl_2$ (0.0127 g, 0.0697 mmol) were mixed in 4 mL DMF. After stirring for 1 hour, the resultant mixture was sealed in a glass vial (20 mL) and heated at 90 °C for 3 days. After cooling to room temperature slowly, orange block crystals were obtained. Yield: about 24 mg (30% based on Mn). IR (solid ATR, ν/cm^{-1}): 3051 (w), 1637 (m), 1596 (m), 1052 (s), 904 (vs), 638 (vs), 565 (w).

$(MV)_2[Cu(DMF)_2](MnMo_6O_{18}L_2)_2 \cdot 6DMF$ (2): 2 was synthesized using the same process to that of **1**, except CuI (0.0358 g, 0.1880 mmol) was used as additional starting material. Transparent block crystals can be obtained (yield: 10.2 mg, 30% based on Mn). IR (solid ATR, ν/cm^{-1}): 3051 (w), 2930 (w), 1643 (s), 1423 (m), 1324 (s), 1056 (s), 910 (s), 655 (s), 555 (m).

$(MV)_2(Cu_2I_3)(MnMo_6O_{18}L_2) \cdot 4CH_3CN$ (3): 3 was prepared under the same conditions with that of 2, except that acetonitrile (4 mL) was used as solvent insteat of DMF. Brown block crystals with yield of 30% (based on Mn, 26.7 mg) can be obtained. IR (solid ATR, ν/cm^{-1}): 3356 (w), 3046 (w),

2958 (w), 2923 (w), 1637 (vs), 1559 (s), 1494 (s), 1430 (s),1324 (s), 1268 (s),1187 (m), 1055 (s), 917(s), 815 (s), 655 (s), 558 (m).

X-ray single crystal diffraction

X-ray diffraction data was collected on a Bruker APEX II CCD area diffractometer equipped with a fine focus, 2.0 kW sealed tube X-ray source (Mo Kα radiation, λ = 0.71073 Å) at 175(2) K. During the data reduction, multi-scan absorption correction (SADABS) including corrections for Lorentz and polarization effects has applied. Crystal structure was solved by the direct method with program SHELXS and refined with the least-squares program SHELXL.[3] The structures were verified by the ADDSYM algorithm in the PLATON program.[4] The refinement details are summarized in Table S1, selected bond lengths and angles are listed in Table S2, hydrogen bond details are given in Table S3-6. CCDC 2233694-2233696 contains the supplementary crystallographic data for this paper. This data can be obtained free of charge from the Cambridge Crystallographic Data Centre via www.ccdc.cam.ac.uk/data_request/cif.

Device Fabrication

The memory devices with the structures of ITO/active layer/Ag have been fabricated according to previous literature.[5] ITO-coated glass substrate was sequentially cleaned by ultrasonic in acetone, ethanol and deionized water for 20 min, and dried in an oven for 15 min at 110 ˚C. Afterward, 5 mg as-synthesized Anderson-based hybrids hybrids or their precursors (methyl viologen (MV^{2+}), CuI, ($MnMo_6O_{18}L_2$)) were dissolved in 5 mL DMF (concentration: 1 mg/mL). Then 100 μL as-prepared suspension was spin-coated onto ITO substrate. During the spin-coated process, the speed was controlled as follows: 300 rpm for 10 s firstly, and then 2500 rpm for another 40 s. Ag pastes were deposited as the top electrodes through a shadow mask (500 μm width) with circular holes with a diameter about 0.1 cm. Finally, the device was dried at 60˚C for 30 minutes to improve the adhesion.

Section 2: Additional table

Table S1 X-ray crystallographic data in this work

	1	2	3	3-heated
Empirical formula	$C_{84}H_{110}Mn_2Mo_{12}N_{14}O_{52}$	$C_{41}H_{51}CuMn_2Mo_{12}N_6O_{50}$	$C_{48}H_{57}Cu_2I_3MnMo_6N_{10}O_{24}$	$C_{42}H_{48}Cu_2I_3MnMo_6N_6O_{24}$
Formula weight	3409.02	3868.06	2296.42	2159.22
Crystal system	Monoclinic	Triclinic	Triclinic	Triclinic
Space group	$P2_1/n$	*P-1*	*P-1*	*P-1*
a (Å)	22.8412(12)	18.6013(14)	13.4196(16)	13.6009(13)
b (Å)	13.7093(7)	18.6693(15)	13.6602(16)	13.6289(13)
c (Å)	35.3091(16)	23.668(2)	19.687(2)	19.6868(19)
α (°)	90	75.297(3)	72.664(2)	79.229(2)
β (°)	97.084(2)	85.771(3)	79.244(2)	72.871(2)
γ (°)	90	82.235(3)	80.619(2)	80.347(2)
V (Å^3)	10972.2(9)	7870.5(11)	3362.2(7)	3401.2(6)
Z	4	2	2	2
F(000)	6728	3856	2202	2056
ρ_{calcd}(g/cm^3)	2.064	1.632	2.268	2.108
Temperature (K)	175(2)	175(2)	175(2)	175(2)
μ(mm^{-1})	1.642	1.290	3.339	3.292
Refl. Collected	193950	304687	20631	20584
Independent relf.	19417	27982	11410	11785
Parameters	1500	1742	871	764
GOF on F^2	1.038	1.050	0.999	1.021
Final *R* indices (*I*= 2σ(*I*))	R_1=0.0333, wR_2=0.0765	R_1=0.0738, wR_2=0.1964	R_1=0.0534, wR_2=0.0938	R_1=0.0441, wR_2=0.0724
R indices (all data)	R_1=0.0368, wR_2=0.0784	R_1 = 0.0972, wR_2 = 0.2108	R_1=0.1118, wR_2=0.1116	R_1=0.0992, wR_2=0.1121

Table S2 Mn-O bonds in this work (Å)

1	Distance	2	Distance	3	Distance	3-heated	Distance
Mn(1)-O(24)	1.907(3)	Mn(1)-O(19)	2.045(9)	Mn(1)-O(11)#1	1.890(6)	Mn(1)-O(10)	2.013(4)
Mn(1)-O(19)	1.917(3)	Mn(1)-O(20)	1.923(6)	Mn(1)-O(11)	1.890(6)	Mn(1)-O(10)#1	2.013(4)
Mn(1)-O(21)	1.921(3)	Mn(1)-O(21)	1.955(7)	Mn(1)-O(10)#1	1.982(6)	Mn(1)-O(11)	1.969(5)
Mn(1)-O(22)	1.927(3)	Mn(1)-O(22)	2.048(7)	Mn(1)-O(10)	1.982(6)	Mn(1)-O(11)#1	1.969(5)
Mn(1)-O(20)	2.119(3)	Mn(1)-O(23)	1.932(6)	Mn(1)-O(12)#1	2.090(6)	Mn(1)-O(12)	1.959(4)
Mn(1)-O(23)	2.122(3)	Mn(1)-O(24)	1.967(7)	Mn(1)-O(12)	2.090(6)	Mn(1)-O(12)#1	1.959(4)
Mn(2)-O(43)	1.920(3)	Mn(2)-O(43)	1.917(6)	Mn(2)-O(24)	1.973(6)	Mn(2)-O(22)	2.080(5)
Mn(2)-O(47)	1.930(3)	Mn(2)-O(44)	2.086(7)	Mn(2)-O(24)#2	1.973(6)	Mn(2)-O(22)#2	2.080(5)
Mn(2)-O(46)	1.930(3)	Mn(2)-O(45)	1.929(7)	Mn(2)-O(23)	1.978(7)	Mn(2)-O(23)	1.983(5)
Mn(2)-O(44)	1.934(3)	Mn(2)-O(46)	1.929(7)	Mn(2)-O(23)#2	1.978(7)	Mn(2)-O(23)#2	1.983(5)
Mn(2)-O(48)	2.093(3)	Mn(2)-O(47)	2.100(7)	Mn(2)-O(22)	1.987(6)	Mn(2)-O(24)#2	1.897(4)
Mn(2)-O(45)	2.104(3)	Mn(2)-O(48)	1.928(7)	Mn(2)-O(22)#2	1.987(6)	Mn(2)-O(24)	1.897(4)

Symmetry codes for **3**: #1 -x+2,-y,-z+1; #2 -x,-y+2,-z

Table S3 Hydrogen Bonds for 1

D-H···A	D-H/Å	H···A/ Å	D-A/Å	∠(D-H···A)/°	Symmetry code
C(37)-H(37B)···O(49)	0.96	2.38	3.3140(2)	164	
C(37)-H(37C)···O(1)	0.96	2.33	3.1126(2)	138	1/2-x,-1/2+y,1/2-z
C(42)-H(42)···O(35)	0.93	2.26	2.9614(2)	132	
C(44)-H(44)···O(5)	0.93	2.18	3.0779(2)	161	1/2-x,-1/2+y,1/2-z
C(45)-H(45)···O(52)	0.93	2.51	3.3645(2)	152	1/2-x,-1/2+y,1/2-z
C(46)-H(46)···O(50)	0.93	2.33	3.1685(2)	150	1/2-x,-1/2+y,1/2-z
C(47)-H(47)···O(49)	0.93	2.39	3.2784(2)	161	1/2-x,-1/2+y,1/2-z
C(48)-H(48C)···O(52)	0.96	2.57	3.3815(2)	142	1/2-x,-1/2+y,1/2-z
C(49)-H(49B)···O(16)	0.96	2.41	3.1872(2)	137	1-x,1-y,1-z
C(49)-H(49C)···O(17)	0.96	2.44	3.1223(2)	128	
C(50)-H(50)···O(37)	0.93	2.53	3.3048(2)	141	1/2-x,1/2+y,1/2-z
C(51)-H(51)···O(50)	0.93	2.56	3.4145(2)	153	1/2-x,-1/2+y,1/2-z
C(54)-H(54)···O(18)	0.93	2.21	3.0606(2)	152	1-x,1-y,1-z
C(56)-H(56) ···O(40)	0.93	2.43	3.0560(2)	125	1/2-x,1/2+y,1/2-z
C(57)-H(57)···O(29)	0.93	2.44	3.3081(2)	156	1/2-x,-1/2+y,1/2-z
C(58)-H(58)···O(13)	0.93	2.38	3.2462(2)	155	1-x,-y,1-z
C(58)-H(58)···O(14)	0.93	2.48	3.1910(2)	133	1-x,-y,1-z
C(60)-H(60A)···O(14)	0.96	2.26	3.1581(2)	156	1-x,-y,1-z
C(60)-H(60B)···O(27)	0.96	2.23	3.0997(2)	150	1/2-x,-1/2+y,1/2-z
C(61)-H(61)···O(30)	0.93	2.5	2.8556(2)	103	
C(62)-H(62)···O(26)	0.93	2.33	3.2330(2)	165	1-x,-y,-z
C(64)-H(64)···O(11)	0.93	2.48	3.1653(2)	130	
C(65)-H(65)···O(9)	0.93	2.44	3.2101(2)	141	
C(67)-H(67)···O(25)	0.93	2.31	3.0320(2)	134	1-x,-y,1-z
C(69)-H(69)···O(6)	0.93	2.32	3.1333(2)	147	x,-1+y,z
C(70)-H(70)···O(4)	0.93	2.51	3.2240(2)	133	x,-1+y,z
C(71)-H(71C)···O(12)	0.96	2.43	3.1811(2)	135	3/2-x,-1/2+y,1/2-z
C(74)-H(74)···O(29)	0.93	2.56	3.3386(2)	141	
C(76)-H(76C)···O(32)	0.96	2.43	3.3381(2)	158	3/2-x,-1/2+y,1/2-z
C(81)-H(81)···O(8)	0.93	2.48	3.3099(2)	148	
C(82)-H(82A)···O(8)	0.96	2.52	3.3632(2)	147	
C(83)-H(83A)···O(13)	0.96	2.49	3.3218(2)	145	3/2-x,1/2+y,1/2-z

Table S4 Hydrogen Bonds for 2

D-H…A	D-H/Å	H…A/ Å	D-A/Å	∠(D-H…A)/°	Symmetry code
C(42)-H(42A)···O(17)	0.96	2.45	3.3973(3)	170	x,1+y,-1+z
C(42)-H(42B)···O(17)	0.96	2.45	3.3485(3)	156	1-x,1-y,1-z
C(43)-H(43)···O(14)	0.93	2.4	3.1633(3)	139	x,1+y,-1+z
C(43)-H(43)···O(15)	0.93	2.56	3.2369(3)	130	x,1+y,-1+z
C(44)-H(44)···O(52)	0.93	2.33	3.2463(3)	170	1-x,1-y,-z
C(46)-H(46)···O(1)	0.93	2.55	3.1777(3)	125	1-x,1-y,1-z
C(47)-H(47)···O(17)	0.93	2.34	3.1897(3)	152	1-x,1-y,1-z

C(51)-H(51)···O(53)	0.93	2.28	3.1163(3)	150	
C(53)-H(53A)···O(34)	0.96	2.34	3.2762(3)	164	-x,1-y,1-z
C(58)-H(58)···O(2)	0.93	2.49	3.3616(3)	156	
C(58)-H(58)···O(4)	0.93	2.56	3.1191(3)	119	
C(62)-H(62)···O(28)	0.93	2.35	3.0881(3)	137	-x,1-y,1-z
C(63)-H(63A)···O(56)	0.96	2.5	3.0884(3)	120	
C(64)-H(64)···O(57)	0.93	2.28	3.0234(3)	136	
C(66)-H(66A)···O(40)	0.96	2.47	3.4022(3)	164	-x,1-y,1-z
C(70)-H(70A)···O（60）	0.96	2.54	3.2251(3)	128	-1+x,y,1+z
C(71)-H(71)···O(25)	0.93	2.6	3.5285(3)	177	
C(74)-H(74)···O(39)	0.93	2.5	3.4088(3)	166	x,1+y,-1+z
C(76)-H(76B)···O(37)	0.96	2.56	3.4700(3)	157	x,1+y,-1+z
C(77)-H(77)···O(14)	0.93	2.4	3.1612(3)	139	
C(78)-H(78B)···O(58)	0.96	2.56	3.4557(3)	155	
C(83)-H(83)···O(31)	0.93	2.4	3.2936(3)	162	-x,1-y,1-z
C(86)-H(86)···O(4)	0.93	2.56	3.3764(3)	147	
C(86)-H(86)···O(6)	0.93	2.54	3.3329(3)	144	
C(88)-H(88C)···O(25)	0.96	2.51	3.2654(3)	136	1-x,1-y,1-z
C(90)-H(90B)···O(36)	0.96	2.59	3.4675(3)	152	-x,1-y,1-z
C(92)-H(92)···O(54)	0.93	2.47	3.3777(3)	166	1-x,1-y,-z

Table S5 Hydrogen Bonds for 3

D-H…A	D-H/Å	H…A/ Å	D-A/Å	∠(D-H…A)/°	Symmetry code
C(24)-H(24)···O(14)	1.09	2.52	3.1064(4)	113	-x,2-y,1-z
C(24)-H(24)···O(16)	1.09	2.19	3.1799(4)	150	-x,2-y,1-z
C(27)-H(27)···N(8)	1.13	2.19	3.2355(4)	153	
C(31)-H(31A)···I(1)	0.96	3.01	3.8732(5)	151	1-x,1-y,1-z
C(31)-H(31B)···O(14)	0.96	2.47	3.3290(4)	149	-x,2-y,1-z
C(32)-H(32)···O(6)	0.93	2.5	2.9000(3)	106	-1+x,1+y,z
C(32)-H(32)···I(1)	0.93	2.96	3.7020(4)	138	1-x,1-y,1-z
C(35)-H(35)···N(7)	0.93	2.57	3.1167(4)	118	-1+x,1+y,z
C(36)-H(36)···O(14)	0.93	2.31	3.1784(4)	155	-x,2-y,1-z
C(37)-H(37A)···O(3)	0.96	2.42	3.2960(4)	151	-1+x,1+y,z
C(37)-H(37B)···O(5)	0.96	2.37	3.3224(4)	174	-x,2-y,1-z
C(38)-H(38)···O(4)	0.93	2.41	3.2470(4)	150	-x,2-y,1-z
C(41)-H(41)···N(10)	0.93	2.46	3.2366(4)	141	
C(43)-H(43A)···O(5)	0.96	2.58	3.4867(4)	157	-1+x,1+y,z
C(45)-H(45A)···I(3)	0.96	3.03	3.8173(5)	140	1-x,-y,1-z
C(45)-H(45B)···O(19)	0.96	2.46	3.3127(4)	148	-x,1-y,1-z
C(47)-H(47A)···O(2)	0.96	2.5	3.4104(4)	158	-x,2-y,1-z
C(47)-H(47B)···O(15)	0.96	2.21	3.0909(4)	151	1-x,1-y,1-z

Table S6 Hydrogen Bonds for 3 after heating

D-H…A	D-H/Å	H…A/ Å	D-A/Å	∠(D-H…A)/°	Symmetry code
C(26)-H(26)···O(1)	0.93	2.53	3.1061(3)	121	
C(26)-H(26)···O(8)	0.93	2.36	3.1606(3)	144	

C(30)-H(30A)···O(14)	0.96	2.54	3.1868(3)	125	1-x,2-y,-z
C(30)-H(30C)···O(1)	0.96	2.45	3.3089(3)	148	1-x,1-y,1-z
C(31)-H(31)···O(1)	0.93	2.32	3.1956(3)	156	1-x,1-y,1-
C(35)-H(35)···I(2)	0.93	2.97	3.7369(4)	141	
C(35)-H(35)···O(21)	0.93	2.51	2.8789(3)	104	1-x,2-y,-z
C(36)-H(36A)···O(20)	0.96	2.59	3.4400(3)	147	1-x,1-y,-z
C(36)-H(36B)···O(20)	0.96	2.52	3.3590(3)	145	1+x,y,z
C(41-)H(41)···O(19)	0.93	2.47	3.3222(3)	152	1+x,y,z

Table S7 RS parameters of memory devices in this work

Devices	V_{Set} /V	V_{Reset} /V	I_{ON}/A	I_{OFF}/A	ON/ OFF ratio
ITO/MV·2I/Ag	2.14	-3.04	1.58×10^{-4}	1.33×10^{-4}	1.19
ITO/CuI/Ag	0.28	-1.98	1.48×10^{-4}	1.17×10^{-4}	1.26
ITO/$MnMo_6O_{18}L_2$/Ag	0.42	-2.33	1.51×10^{-4}	1.89×10^{-5}	7.99
ITO/**1**/Ag	1.39	-2.53	1.84×10^{-4}	1.55×10^{-5}	12.88
ITO/**2**/Ag	1.42	-3.56	1.98×10^{-4}	2.87×10^{-6}	64.69
ITO/**3**/Ag	0.97	-3.49	1.17×10^{-4}	5.01×10^{-7}	2.32×10^{2}
ITO/**3**/Ag after 11 months	0.92	-3.45	1.77×10^{-4}	5.97×10^{-7}	2.96×10^{2}
ITO/**3**/Ag at 240°C	0.96	3.50	2.52×10^{-4}	4.06×10^{-7}	6.21×10^{2}

Table S8 The comparison with relative POM-based memristors

Devices structure	ON/OFF ratio	V_{Set}/V_{Reset}/V	Endurance	Retention(s)	Ref.
ITO/ $Na_6V_{10}O_{28}$/Cr/Au	25	1.2/0.8	200	2200	6
ITO/$H_3PW_{12}O_{40}$@PMMA/Au	6×10^{2}	1.2/-1.71	100	10^{4}	7
ITO/PMMA– MAPOM/Pt	4~5	1.0/1.5/-1.35	50	10^{4}	8
ITO/$[Co(H_2O)_6]_2[Co_3(bpdo)_4(H_2O)_{10}][Co_4(H_2O)_2$(B-a-$PW_9O_{34})_2]\cdot2$ bpdo$\cdot14H_2O$ /Ag	55.5	-0.63/0.75	20	-	9
ITO/$\{[Co_2(bpdo)_4(H_2O)_6](\alpha\text{-}GeW_{12}O_{40})\}\cdot4(H_2O)\}_n$ /Ag	1.0×10^{2}	1.77/−3.42	100	-	5
ITO/$(MV)_3(MnMo_6O_{18}L_2)_2\cdot4$DMF /Ag	12.88	1.39/-2.53	20	-	this work
ITO/$(MV)_2[Cu(DMF)_2](MnMo_6O_{18}L_1)_2\cdot6$DMF/Ag	64.69	1.42/-3.56	84	-	this work
ITO/$(MV)_2[Cu_2I_3](MnMo_6O_{18}L_2)\cdot4CH_3CN$ /Ag	2.32×10^{2}	0.97/-3.49	700	10^{4}	this work

Section 3: Additional structural figures and characterizations

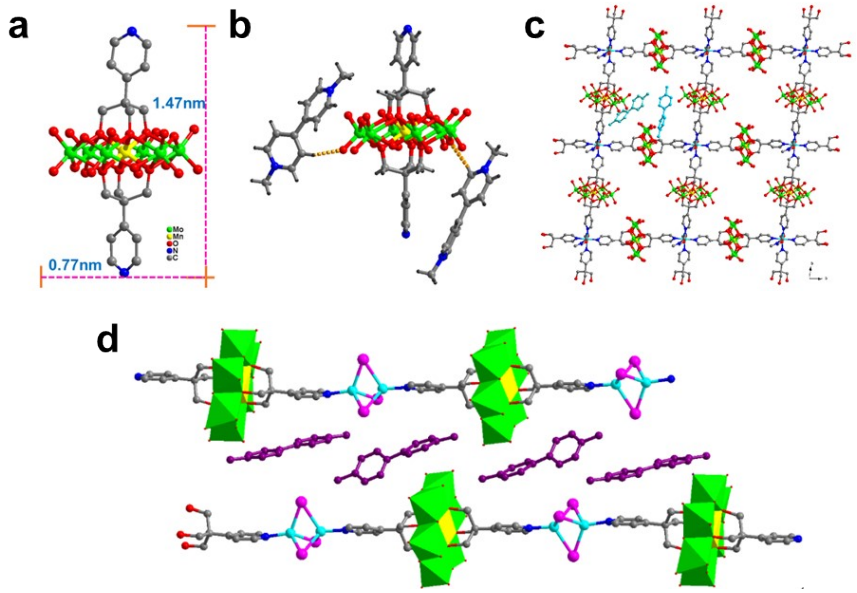

Fig. S1 (a) The structure of $(MnMo_6O_{18}L_2)^{3-}$ unit; (b) hydrogen bonds between $(MnMo_6O_{18}L_2)^{3-}$ and MV^{2+} cations in **1**; (c) 2D layer of **2** showing the position of MV^{2+}; (d) the encapsulation of MV^{2+} into the 1D $[(Cu_2I_3)(MnMo_6O_{18}L_2)]_n^{2n-}$ chains.

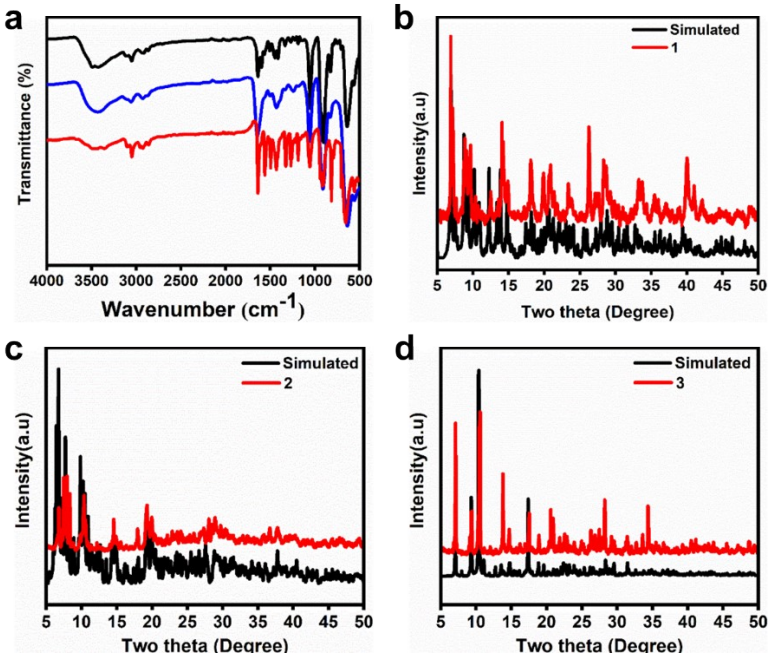

Fig. S2 (a) IR spectra of three hybrids; Simulated and experiment PXRD patterns: (b) **1**; (c) **2**; (d) **3**.

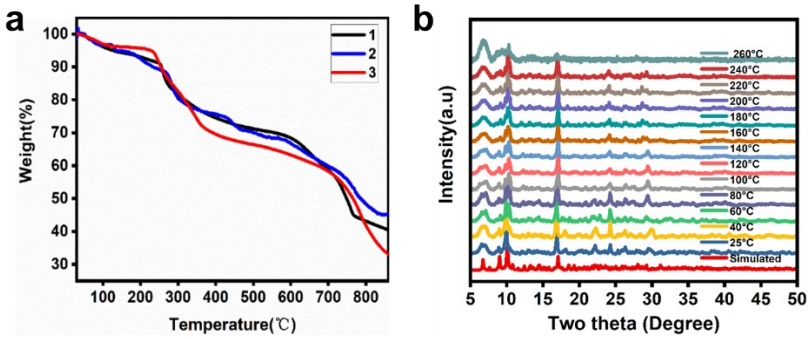

Fig. S3 (a) TG curves of **1**, **2** and **3**; (b) simulated and temperature-dependent PXRD patterns of **3**.

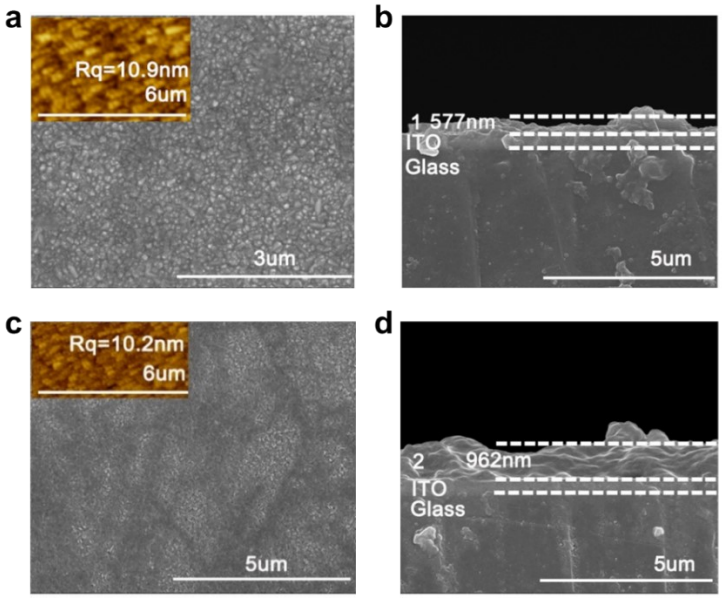

Fig. S4 The top-view (inserted: the surface AFM image) and the cross-sectional SEM images showing the thickness: (a, b) ITO/**1**/Ag; (c, d) ITO/**2**/Ag.

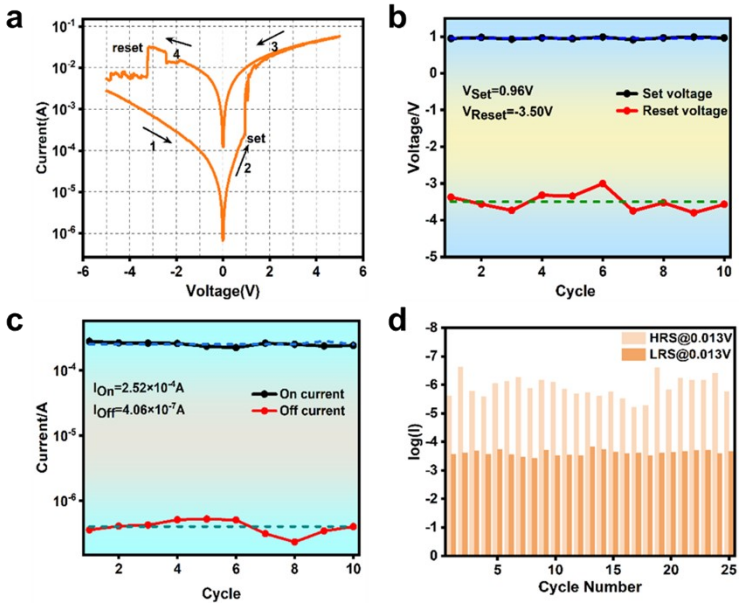

Fig. S5 Device stability of ITO/**3**/Ag at 240 °C: (a) *I-V* curves; (b) the V_{Set}/V_{Reset} showing random 10 cycles; (c) I_{ON} and I_{OFF} showing random 10 cycles; (d) cycle endurance showing 25 cycles.

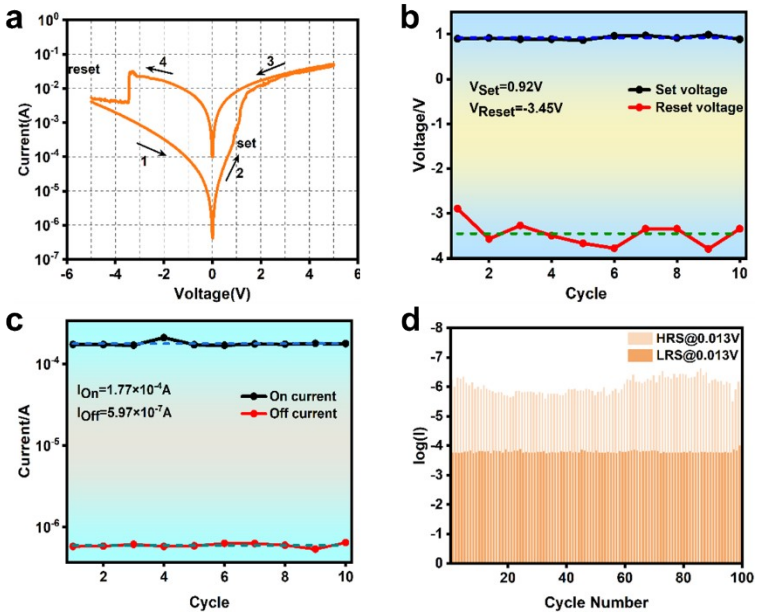

Fig. S6 Device stability of ITO/**3**/Ag after one year: (a) *I-V* curves showing four sweeping ranges; (b) the V_{Set}/V_{Reset} distribution with random 10 cycles; (c) I_{ON} and I_{OFF} showing random 10 cycles; (d) cycle endurance with 100 cycles.

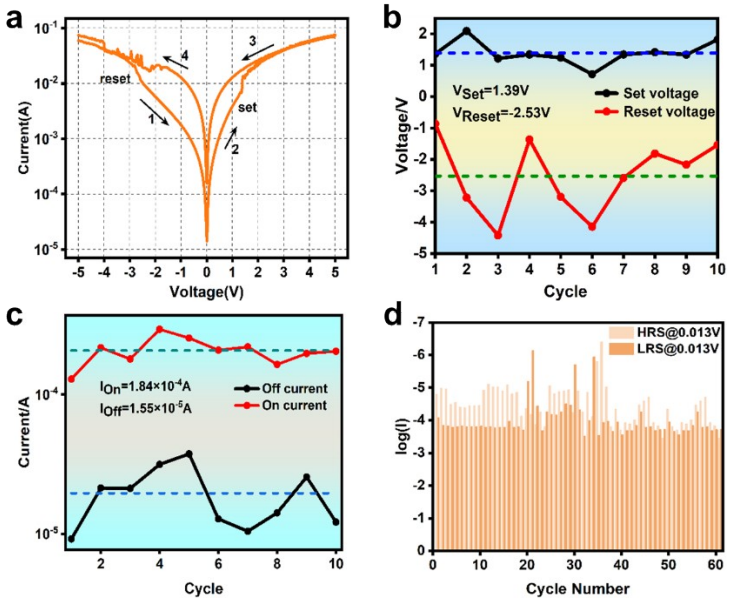

Fig. S7 (a) *I-V* curves of the ITO/**1**/Ag showing four sweeping processes; (b) the averaged V_{Set}/V_{Reset} calculated from 10 cycles; (c) the averaged HRS and LRS currents calculated from 10 cycles; (d) cycle endurance of the ITO/**1**/Ag device by showing 65 cycles.

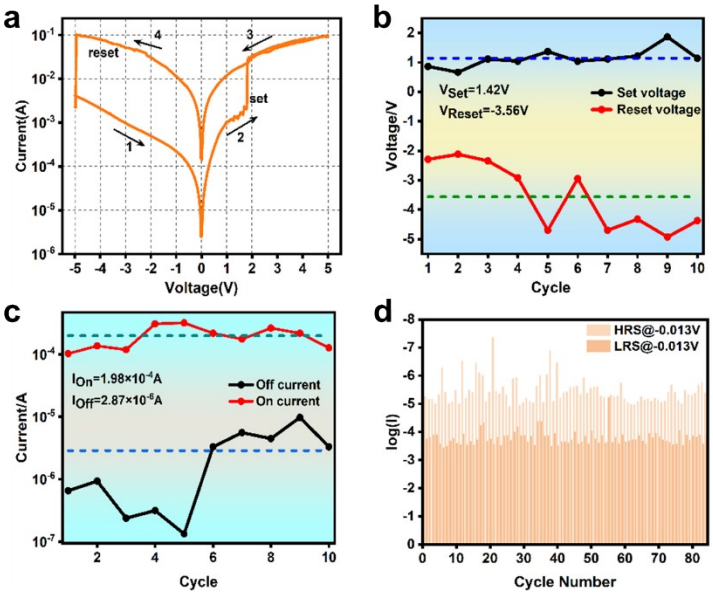

Fig. S8 (a) *I-V* curves of the ITO/**2**/Ag device showing four sweeping processes; (b) the averaged V_{Set}/V_{Reset} calculated from 10 cycles; (c) the averaged HRS and LRS currents calculated from 10 cycles; (d) cycle endurance of the ITO/**2**/Ag device showing 90 cycles.

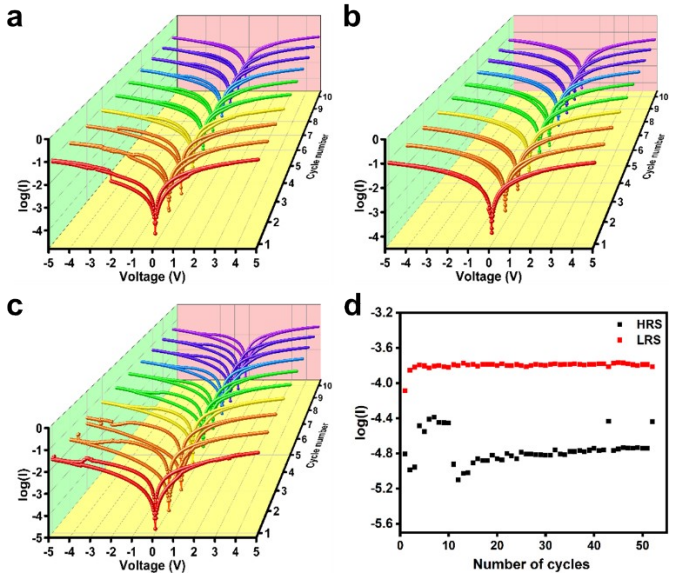

Fig. S9 (a) *I-V* curves of the ITO/MV·2I/Ag device with 10 cycles; (b) *I-V* curves of the ITO/CuI/Ag device with 10 cycles; (c) *I-V* curves of the ITO/$MnMo_6O_{18}L_2$/Ag device with 10 cycles; (d) HRS and LRS of ITO/$MnMo_6O_{18}L_2$/Ag device.

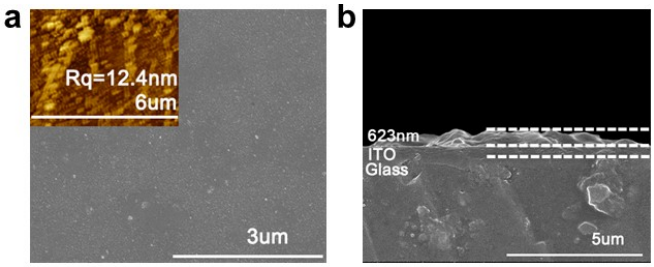

Fig. S10 SEM image of ITO/$MnMo_6O_{18}L_2$/Ag: (a) top-view SEM image (inserted: the surface AFM image); (b) the cross-sectional image showing the thickness

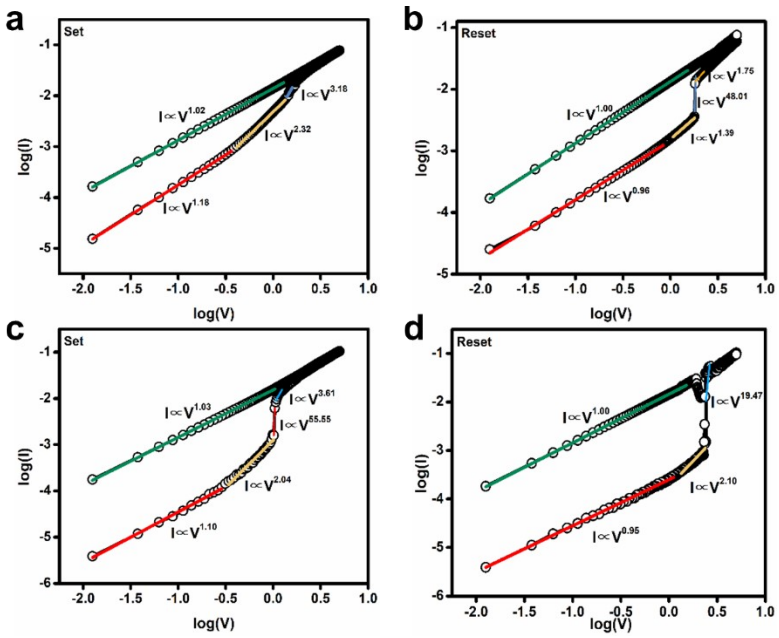

Fig. S11 Log-log plots on the *I-V* curves: (a) ITO/**1**/Ag during Set process; (b) ITO/**1**/Ag during Reset process; (c) ITO/**2**/Ag under during Set process; (d) ITO/**2**/Ag during Reset process.

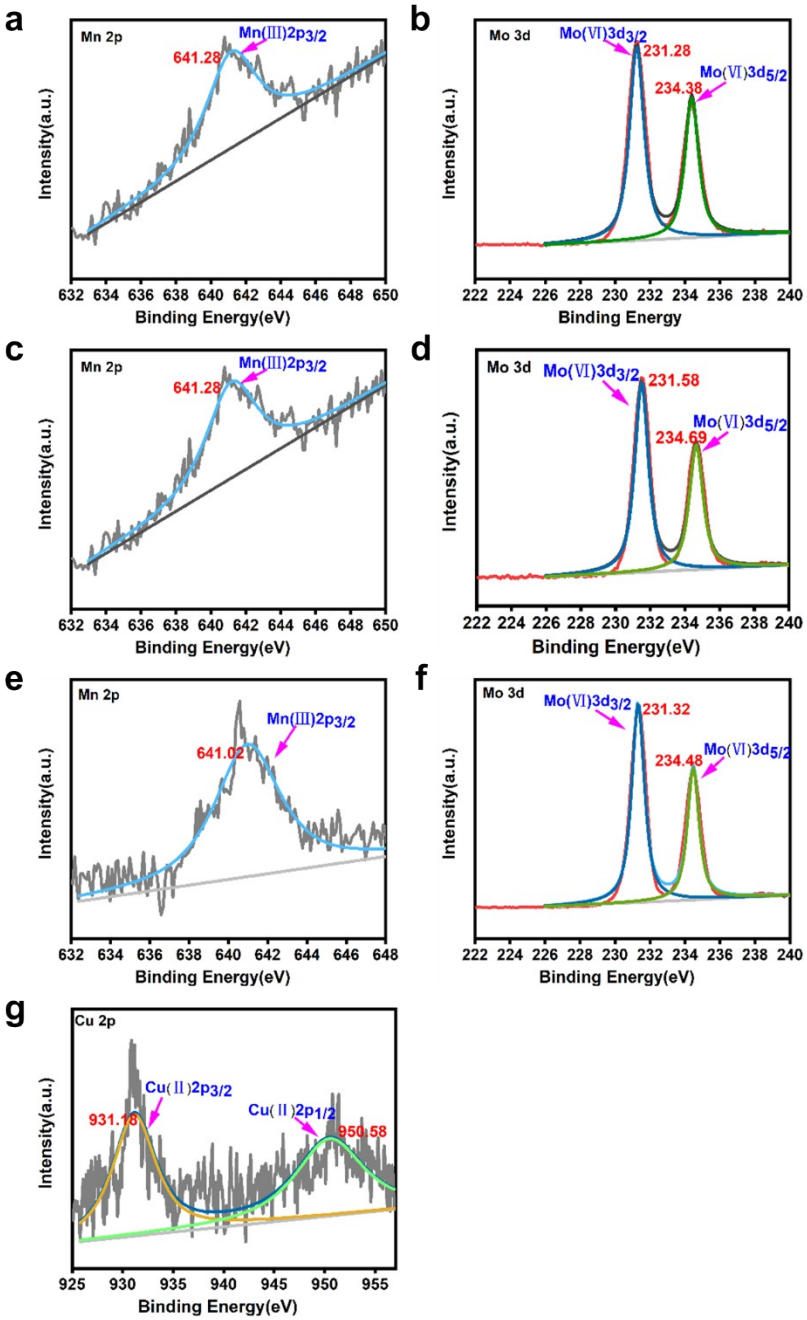

Fig. S12 The XPS spectra: (a) Mn-2p and (b) Mo-3d for $MnMo_6O_{18}L_2$; (c) Mn-2p and (d) Mo-3d for **1**; (e) Mn-2p and (f) Mo-3d for **2**; (g) Cu-2p for **2**.

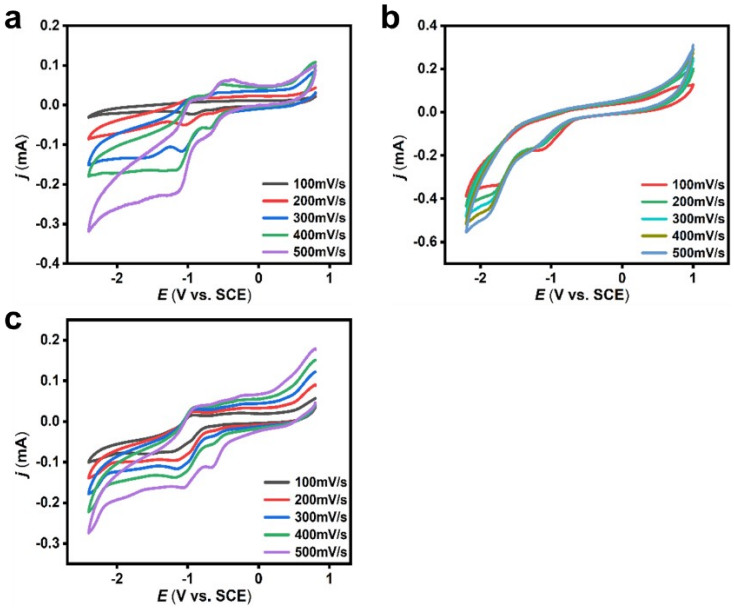

Fig. S13 Cyclic voltammogram (CV) of three hybrids with different scanning rates: (a) **1**; (b) **2**; (c) **3.**

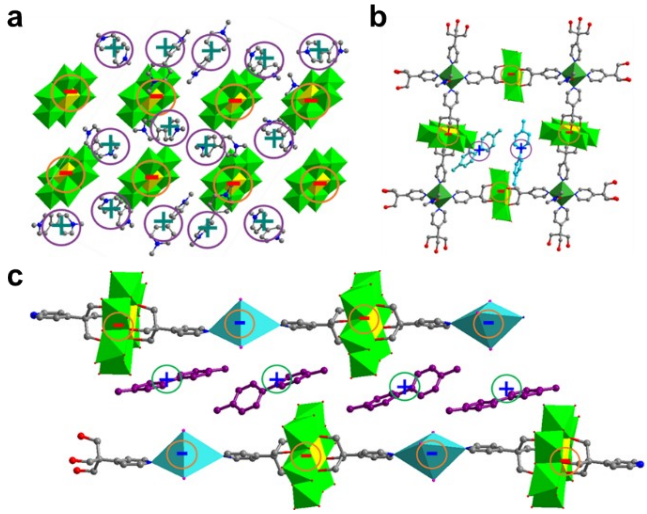

Fig. S14 The packing diagram showing the positions of electron-rich POM/Cu_2I_3 clusters and electron-poor MV^{2+}: (a) **1**; (b) **2**; (c) **3**.

References

1 X. Li, Y. Wang, R. Wang, C. Cui, C. Tian and G. Yang, *Angew. Chem. Int. Ed. Engl.* 2016, **55**, 6462–6466.

2 D. Menozzi, E. Biavardi, C. Massera, F. Schmidtchen, A. Cornia and E. Dalcanale, *Supramol. Chem.* 2010, **22**, 768–775

3 G. A. Sheldrick, A short history of SHELX, *Acta Crystallogr. Sect. A* 2008, **64**, 112–122.

4 A. Spek, Single-crystal structure validation with the program PLATON, *J. Appl. Crystallogr.* 2003, **36,** 7–13.

5 B. Chen, Y. Huang, K. Song, X. Lin, H. Li and Z. Chen, *Chem. Mater.* 2021, **33**, 2178−2186.

6 N. S. Sterin, B. Nivedita, C. Marc, M. N. Satyanarayan, S. M. Sib and P. D. Partha, *Phys. Status Solidi A.* 2020, **217**, 2000306.

7 X. Chen, P. Huang, X. Zhu, S. Zhuang, H. Zhu, J. Fu, A. Nissimagoudar, W. Li, X. Zhang, L. Zhou, Y. Wang, Z. Lv, Y. Zhou and S. Han, *Nanoscale Horiz.* 2019, **4**, 697–704.

8 B. Hu, C. Wang, J. Wang, J. Gao, K. Wang, J. Wu, G. Zhang, W. Cheng, B. Venkateswarlu, M. Wang, P. Lee and Q. Zhang, *Chem. Sci.* 2014, **5**, 3404–3408.

9 Y. Huang, X. Lin, B. Chen, H. Zheng, Z. Chen, H. Li and S. Zheng, *Angew Chem. Int. Ed. Engl.* 2021, **60**, 16911–16916.